

An optical and near-infrared multipurpose instrument HONIR

Kiyoshi Sakimoto^a, Hiroshi Akitaya^b, Takuya Yamashita^c, Koji S. Kawabata^b, Hidehiko Nakaya^c, Hisashi Miyamoto^d, Tatsuya Harao^a, Ryosuke Itoh^a, Risako Matsui^a, Yuki Moritani^b, Asami Nakashima^{e,c}, Takashi Ohsugi^{b,a}, Mahito Sasada^f, Katsutoshi Takaki^a, Issei Ueno^a, Takahiro Ui^{a,c}, Takeshi Urano^a, and Michitoshi Yoshida^b

^aDepartment of Physical Science, School of Science, Hiroshima University, Kagamiyama 1-2-1, Higashi-Hiroshima 739-8526, JAPAN;

^bHiroshima Astrophysical Science Center, Hiroshima University, Kagamiyama 1-2-1, Higashi-Hiroshima 739-8526, JAPAN;

^cNational Astronomical Observatory of Japan, Osawa 2-21-1, Mitaka, Tokyo 181-8588, JAPAN;

^dMolex Japan Co., Ltd., Fukami-Higashi 1-5-4, Yamato, Kanagawa 242-8585, JAPAN;

^eDepartment of Astronomy, Graduate School of Science, The University of Tokyo, Hongo 7-3-1, Bunkyo-ku, Tokyo 113-8656, JAPAN;

^fDepartment of Astronomy, Kyoto University, Kitashirakawa-Oiwake-cho, Sakyo-ku, Kyoto 606-8502, JAPAN

ABSTRACT

We have developed an optical-infrared instrument HONIR (Hiroshima Optical and Near-InfraRed camera) to be attached to the 1.5-m Kanata telescope at Higashi-Hiroshima Observatory, Hiroshima University. HONIR is a three color (one optical and two near-infrared bands among 0.5–2.4 μm) simultaneous imager and spectrograph with a polarimetry function. The field of view of the imaging mode is 10 arcmin square with a spatial sampling of $0''.29$. Among the planned multipurpose functions, a two color (0.5–1.0 μm and 1.15–2.40 μm) simultaneous imaging function has been installed and operated so far. The remaining functions, spectroscopy and polarimetry, and the second near-infrared band arm, are under development and will be installed in the near future.

Keywords: optical, infrared, imaging, spectroscopy, polarimetry

1. INTRODUCTION

We have developed a new instrument HONIR (Hiroshima Optical and Near-InfraRed camera) to be attached on the Kanata telescope at Higashi-Hiroshima Observatory.

The Kanata telescope is a 1.5-m diameter Ritchey-Chretien telescope at Higashi-Hiroshima Observatory managed by Hiroshima Astrophysical Science Center, Hiroshima University. On the telescope, three focal ports, one Cassegrain port and two Nasmyth ports, are available (Table 1). We have operated sophisticated instruments on the telescope: TRISPEC¹ capable of imaging, spectroscopy, and polarimetry, at three bands among optical and near-infrared wavelengths simultaneously, and HOWPol² capable of optical imaging, spectroscopy, and Stokes Q-U simultaneous polarimetry. By use of these instruments, with a tight collaboration with high-energy satellites, we have published many observational results especially on variable objects such as blazars, super novae, and gamma-ray bursts.^{3–7}

Further author information: (Send correspondence to H. Akitaya)

H. Akitaya : E-mail: akitaya@hiroshima-u.ac.jp, Telephone: +81 82 424 5765, Fax: +81 82 424 5765

Table 1. Basic parameters of the Kanata telescope.

Type	Ritchy-Cretien
Primary mirror diameter	1.5 m
Focal number	F/12.3
Plate scale	11.148 arcsec/mm
Field of view	15 arcmin
Focal ports: Instrument	Cassegrain (with an instrumental rotator): HONIR Nasmyth #1 (with an instrumental rotator): HOWPol Nasmyth #2: High-speed camera, etc.

HONIR is a brand-new instrument for the Kanata telescope that takes over and upgrades multipurpose capabilities of the previous instrument TRISPEC. It is designed as an imager and spectrograph with a polarimetry function that obtains three band information among optical-infrared wavelengths of 0.5–2.4 μm simultaneously with a field of view of 10 arcmin square.

We started its development in early 2007 and conducted the first test operation on the telescope with one near-infrared imager in 2009. In the recent observational runs from October 2011, we installed a function of two bands (one optical and one near-infrared) simultaneous imaging and started its operation.

In the near future, functions of spectroscopy and polarimetry (imaging polarimetry and spectro-polarimetry) will be installed. In addition, another near-infrared arm will be also appended, which enables us to perform three (one optical and two near-infrared) bands simultaneous observation.

In this paper, we introduce a concept of the instrument. We also report the current status and initial accomplishments that had been performed in the recent observational runs with the existing function of two band simultaneous imaging.

2. DESIGN AND SPECIFICATIONS

HONIR is to be attached on the Cassegrain focus of the Kanata telescope. HONIR is designed to obtain images of three wavelength bands (ranges of 0.5–1.0 μm , 1.15–1.35 μm , and 1.45–2.40 μm) simultaneously with a field of view of 10 arcmin by 10 arcmin. In addition to imaging, spectroscopy and combination use of polarimetry are also available. All of the optical components in the instrument after the entrance optical window are mounted on the optical bench cooled down to around 60–70 K in a vacuum chamber.

Among the planned functions in the design, that of two bands (wavelength ranges of 0.5–1.0 μm and 1.15–2.40 μm) simultaneous imaging has been installed so far. The remaining functions (spectroscopy, polarimetry, and the second near-infrared band arm) will be added in the near future. The basic specifications of the instrument are summarized in Table 2.

2.1 Optical Design and Layout

The basic concept of the optics design of HONIR is a reimaging optical system with three branched arms split by two dichroic mirrors, which simultaneously produces three images of different wavelength ranges. The layout of the optics and its picture are shown in Fig. 2–3.

A convergent ray from the telescope, passing through a CaF_2 entrance window of the vacuum chamber, is focused on the telescope focal plane, at which one of the focal masks (a square aperture for imaging, a narrow slit for spectroscopy, etc.) in the rotating turret is placed. An actual size of the whole field of view of $10' \times 10'$ at the telescope focal plane is 53.8 mm by 53.8 mm. It is followed by a common collimator lens unit and a cold stop. The consequential collimated beam incidents a series of dichroic mirrors (Table 3) so that the beam is split into three passes with different wavelength ranges: the optical arm at 0.5–1.0 μm , the IR arm #1 at 1.45–2.40 μm , and the IR arm #2 at 1.15–1.35 μm . Each arm has a camera lens that refocuses a demagnified field image on a detector. We use different types of detector between optical and near-infrared wavelengths: a CCD with a pixel size of 15 μm and a HgCdTe detector with that of 20 μm (See section 2.3). Focal lengths

of the camera lenses and consequent magnification factors of reimaging are tuned so that an image of the whole field of view of $10' \times 10'$ is focused at a pixel scale of 0.29 arcsec/pixel on both the detectors. Each of the collimator lens unit and camera lens units consists of six or seven spherical lenses made of several glass materials and with anti-reflection coating. The properties of the lenses are summarized in Table 4.

It is planned to install three arms finally, however, the IR arm #2 components including its dichroic mirror has not been installed yet. Therefore, the optical arm for 0.5–1.0 μm and the IR arm #1 for 1.15–2.40 μm are available so far.

The optics is designed for operation at 85 K. In the design, an 80% encircled energy is achieved at a radius of $< 17 \mu\text{m}$ at H and K_s bands, $< 12 \mu\text{m}$ at J band, and $< 5.4 \mu\text{m}$ at optical wavelengths, over the whole imaging area on a detector. Distortion of an image on a detector is less than 0.18 % at H and K_s bands, less than 0.19 % at J band, and less than 0.06% at optical wavelengths.

In the near future, the optical components for spectroscopy and linear polarimetry will be installed.

For spectroscopy, a slit mask on the telescope focal plane and gratings in the collimated beam at each arm are inserted. A set of gratings and a slit mask of 0.2 mm (or 2.2 arcsec) width have been designed for low dispersion spectroscopy ($R \sim 350$), which are in the process of production (Table 5). In addition, we are also planning to add gratings with a higher dispersion ($R \sim 700$) and lower dispersion ($R \sim 30$).

The forthcoming polarimetry will be performed by use of a rotatable super-achromatic half-wave plate mounted just above the entrance optical window, an appropriate focal mask or slit at the telescope focal plane, and a Wollaston prism as a polarization beam splitter at the pupil plane. A Wollaston prism splits an incoming beam into two separated ones which are perpendicularly polarized.

We designed the Wollaston prism to satisfy the following requirements: an efficient beam splitting angle (namely a large birefringence of the material and a large wedge angle of the wedge components) to split a

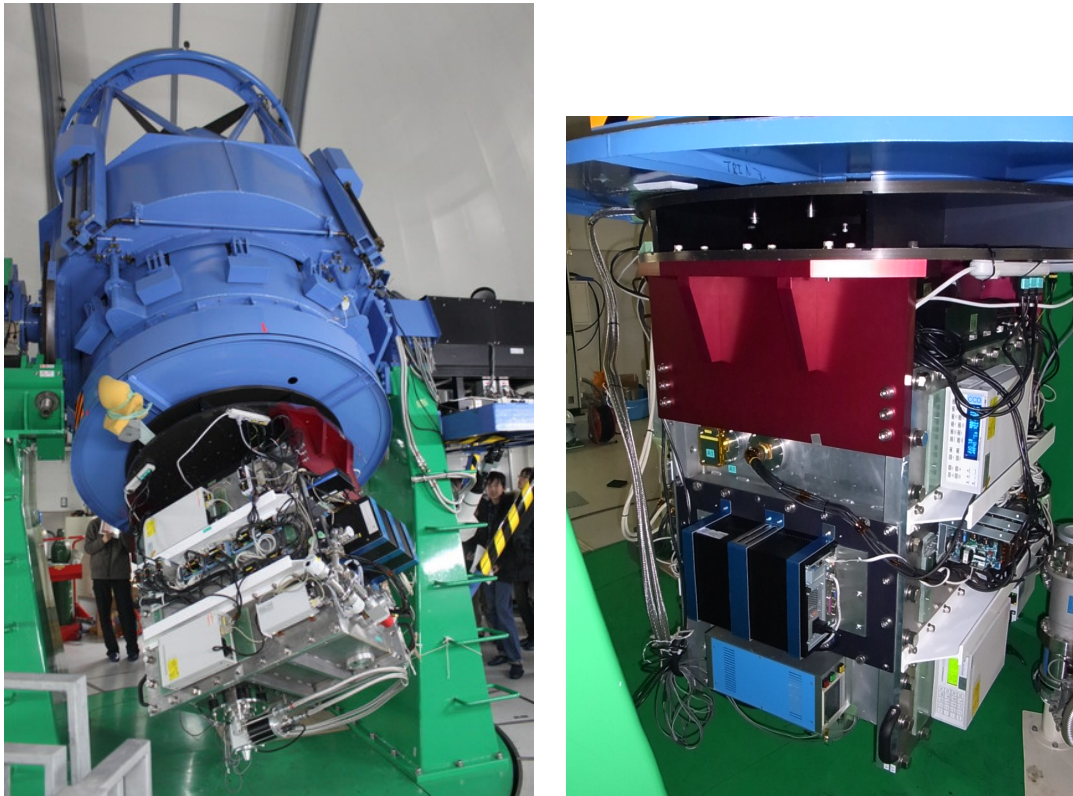


Figure 1. HONIR attached on the Kanata telescope (left) and its closeup (right).

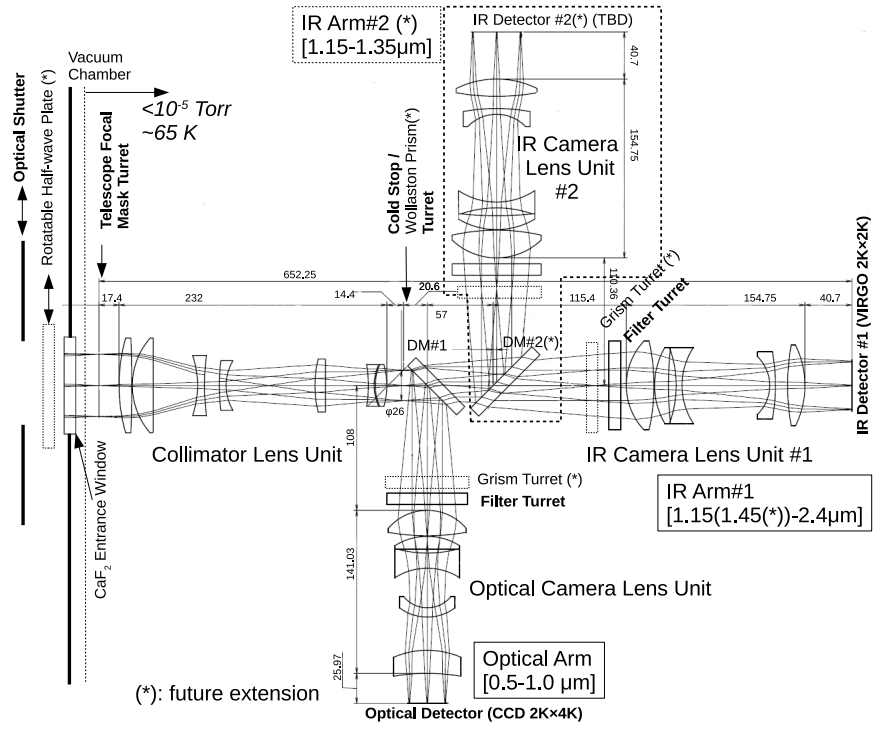


Figure 2. Optical design and layout of HONIR.

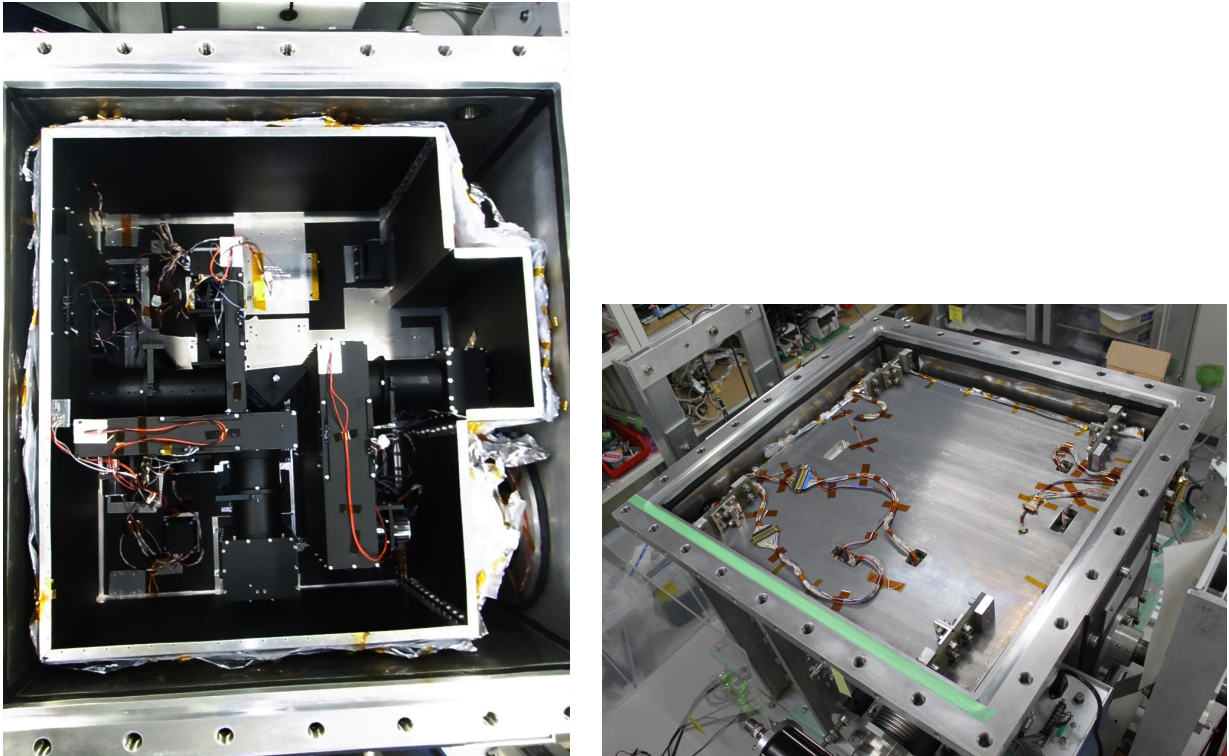


Figure 3. Optical components mounted on the optical bench (left) and its bottom side (right).

Table 2. Basic specifications of HONIR.

Property		Arm		
		Optical	IR #1	IR #2 (in future)
Wavelength coverage (μm)		0.5 ^a –1.0	1.45(1.15) ^b –2.40	1.15–1.35
Field of view (FOV) (arcmin)		10 \times 10	10 \times 10	TBD
Plate scale (arcsec/mm) ^c			11.148	
Size of the whole FOV (mm) ^c			53.8 \times 53.8	
Sampling rate (arcsec/pix) ^d		0.29	0.29	TBD
Size of the whole imaging area (mm) ^d		30.7 \times 30.7	40.9 \times 40.9	TBD
Filters		B ^a , V, R _C , I _C , z', Y	Y, J, H ^e , Ks ^e	H, Ks
Detector	Type	CCD	HgCdTe (VIRGO)	TBD
	Vendor	Hamamatsu Photonics	Raytheon	TBD
	Format (pixels)	2048 \times 4096 ^f	2048 \times 2048	TBD
	Pitch (μm)	15	20	TBD
	Size (mm)	30.72 \times 61.44	40.96 \times 40.96	TBD

^a Partially transparent at 0.4–0.5 μm (B-band).

^b Until the future installation of the IR arm #2.

^c At the telescope focal plane.

^d On the detector.

^e To be moved to the IR arm #2 after its installation.

^f A half of the area is actually used for imaging.

Table 3. Specification of the dichroic mirrors.

Dichroic mirror	Wavelengths (μm)	Efficiency
#1 (optical–IR splitting)	0.50–1.00	> 90% reflectance
	1.00–1.15	transition
	1.15–2.40	> 90% transmittance
#2 (J–H splitting)	1.15–1.35	> 85% reflectance
	1.35–1.45	transition
	1.45–2.40	> 90% transmittance

stellar image efficiently on the detector, a small color dispersion (a small wavelength dependency of a refractive index), a wide range transmittance for all of the wavelengths of 0.5–2.4 μm that HONIR measures, and a small difference of coefficients of thermal expansion between two different optical axes to avoid destruction owing to its cooling. A size constraint is also rigid because of the crowded optical layout. Thus, we have selected LiYF₄ (YLF)^{8,9} as the best material among candidates and designed the Wollaston prism as shown in Table 6 and Fig. 4. The collimated beam is split into two inclined beams with orthogonal linear polarization modes at a separation angle of 0.74–0.77 degrees depending on the wavelength. Consequently, dual stellar images of two linear polarization modes are focused on the detector separated by 46–48 arcsec each other. We also use a focal mask with a series of long rectangular apertures of 600'' \times 45'' placed at a 93 arcsec pitch along the direction of the beam separation, which truncates a half of the whole image area discontinuously as a shape of a barred lattice. As a result, we obtain pairs of orthogonally polarized rectangular images without their overlap. Obtaining a series of polarized images with rotating the half-wave plate at a 22° step, we finally measure the linear polarization distribution in the image. In addition, using an appropriate focal slit mask and grisms together, spectro-polarimetry is also capable. We intend to achieve a polarimetric accuracy of better than 0.1 percent.

Table 4. Construction of the lens units.

Lens unit	Collimator lens	Optical camera lens	IR camera lens ^a
Focal length (mm)	312.0	178.0	237.2
Magnification factor ^a	–	0.5705	0.7603
Plate scale (arcsec/mm) ^b	–	19.55	14.67
Number of lenses	7	5	5
Lens materials	S-FPL53, S-TIH53, S-FTM16, S-FPL51	CaF ₂ , S-FPL53, S-FTM16, S-FPL51	CaF ₂ , S-FPL53, S-FTM16, S-FPL51
Effective diameter (mm)	80	75	75

^a The same configuration for both the IR #1 arm and IR #2 arm.

^b On the detector as a combination with the collimator lens.

Table 5. Design of the gratings for low dispersion spectroscopy.

Arm	Optical	IR #1	IR #2
Wavelength coverage	0.41–0.97	1.50–2.40	1.07–1.43
Slit width (arcsec)		2.2 ^a	
Resolution ($R = \lambda/\Delta\lambda$)	330	371	354
Wavelength of the maximum efficiency (μm)	0.683	1.933	1.232
Material	BK7	S-FTM16	BK7
Wedge angle (degrees)	21.5	22.5	23.5
Grooves (gr/mm)	300	120	180
Blaze angle (degrees)	23.0	26.7	23.9
Groove pattern type ^b	54-039R	54-831R	54-870R
Size (mm)	51×51×21	59×59×26	59×59×27
Effective diameter (mm)	47	55	55

^a 0.2mm at the telescope focal plane.

^b Model number of Richardson Gratings, Newport Corporation.

2.2 Cryogenics

Almost all of the principal components of HONIR are enclosed in a vacuum chamber and cooled down to suitable temperatures to suppress thermal background radiation from the instrument itself and thermal noise of the detectors.

The vacuum chamber is a large box, measuring 960×960×630 mm, built up by welding boards and frames of aluminum base alloy. It was manufactured by TAIYO NIPPON SANSO Corp.

The chamber contains an optical bench, on which lens units, optical elements, and detector containers are mounted. The optical bench is attached to the chamber wall through four non-rigid supports made of glass epoxy and metal plates and enclosed by a radiation shield box for its thermal isolation from the ambient chamber walls. Following evacuation of the chamber by a pressure of $\sim 10^{-3} - 10^{-4}$ Torr, the optical bench is cooled down to and kept at 60–70 K with a refrigerator directly connected to the optical bench. A single stage Gifford-McMahon cycle refrigerator RF-471 by AISIN SEIKI Co.,Ltd., with a cooling power of 140 W at 70 K, is used.

The detectors (CCD and HgCdTe detector) in their container are placed on a cold plate connected to the cooled optical bench through a narrow thermal path. The temperature of each detector is stabilized at the appropriate level for its operation (173 K for the CCD and ~ 75 K for the HgCdTe detector) by use of a platinum thermometers and a resistance heater on the cold plate controlled by a temperature controller (model 331 by Lake Shore Cryogenics, Inc.).

In the recent operation of the instrument at ambient temperatures ranging from -5 to +15 degrees C, it took 100 hours to cool the optical bench from room temperature to 60 K, following 38 hours evacuation of the

Table 6. Design of the Wollaston prism.

Material	LiYF ₄ (YLF)
Number of components	2
Size (mm)	34×34×12
Effective aperture diameter	30 mm
Wedge angle	16°.39
Beam splitting angle	0°.7685 (0.47 μm)–0°.7381 (2.4 μm)
Image separation on the detector	47".80 (0.47 μm)–45".90 (2.4 μm)
Operating temperature	80 K
Wavelength range	0.5–2.4 μm
Wavefront error	λ/2
Other features	Optical contact or adhesive (TBD)

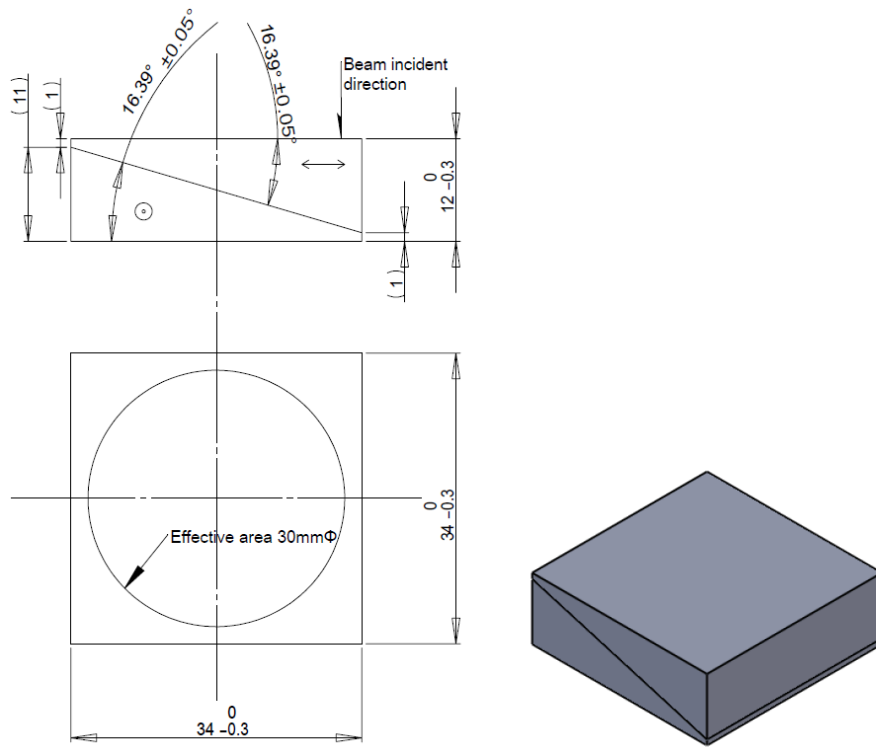


Figure 4. Design of the Wollaston prism.

chamber by a pressure of 2×10^{-3} Torr. The temperature of the optical bench and pressure in the chamber had been kept at 60–70 K and $\leq 10^{-5}$ Torr, respectively, for 36 days at least. In addition, further improvement of the cryogenic performance is planned by installing additional radiation shields and a sorption pump on the cold head of the refrigerator.

2.3 Detectors and Readout Electronics

HONIR equips two detector arrays and their controller systems for the optical arm and the IR arm #1 at present. The block diagram of the detector system is shown in Fig. 5.

For the optical arm, a fully-depleted back-illuminated CCD array with 2048×4096 pixels at a $15 \mu\text{m}$ pitch, manufactured by Hamamatsu Photonics K. K.,¹⁰ is placed. Readout operation is conducted by the integrated control system *Messia 5*,¹¹ and the front-end electronics *MFront2*.^{12,13} The detector temperature is stabilized at 173 K by the cryogenic system. The active detector area has a 1:2 ratio rectangular shape, however, only a half of the area is actually used for the imaging. Signals on pixels in four separated areas are read out in parallel at 133 kHz. A frame readout rate is 17.4 sec/frame for reading the whole pixels including prescan and overscan pixels. A conversion factor is in a range of 1.54–2.15 electrons/ADU depending on the read out ports. The readout noise is ~ 8 electrons rms at the above readout rate.

For the IR #1 arm, one HgCdTe VIRGO-2K focal plane array with 2048×2048 pixels at a $20 \mu\text{m}$ pitch, manufactured by Raytheon Company, is installed at present. The detector is cooled to around 75 K. Its readout is also operated by the *Messia 5* control system, with the multi-array control system *MACS2*¹⁴ as a front-end electronics. The signals from four separate areas on the detector are read out in parallel at a rate of 236 kHz, and consequently a frame rate becomes 4.5 sec/frame to read out 2072×2050 pixels in total including six reference pixels for each row and two reference rows. A conversion factor derived by measuring a photon transfer curve in a laboratory environment is 3.4 electrons/ADU. The signal response against incident light is not deviated from an ideal linear relation by 1 % until 130,000 electrons accumulation. The dark current is at a negligible level of lower than 0.1 electrons/sec. However, the readout noise is at very high level: 24–78 electrons rms (depending on reading ports) at a laboratory and 170–210 electrons rms on the telescope at present. This significant readout noise has restricted detecting faint objects, and should be suppressed.

We are now developing a new readout electronic system for the VIRGO detector to replace the current system. Its design is based on the Kiso Control Array operated on a newly developed Kiso Wide Field Camera¹⁵ at Kiso Schmidt Telescope. The new system will have a function of 16 ports parallel readout, which reduces a frame rate by 1.2 sec/frame and improves efficiency of data acquisition. The reduction of the readout

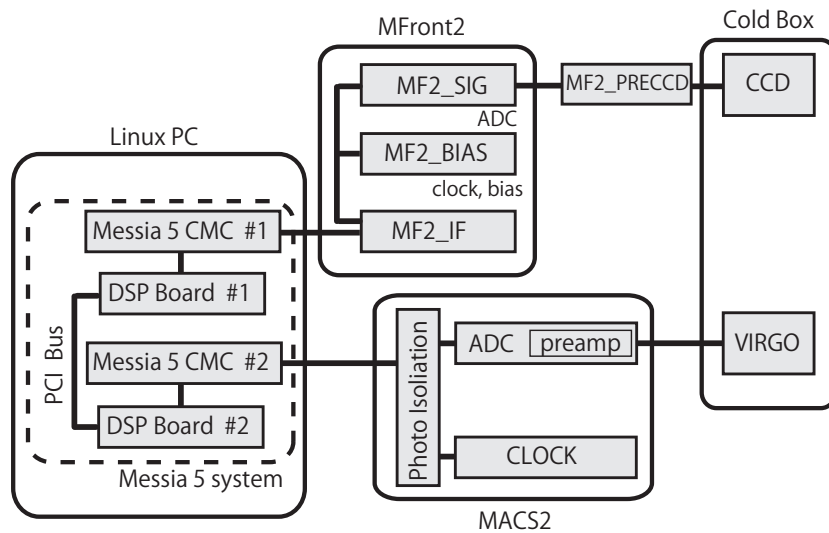


Figure 5. Block diagram of the detector system.

noise is also expected. In the near future, another set of an infrared detector and a readout system will be also installed for the planned additional IR arm #2.

2.4 Mechatronics Design

HONIR has four rotating turrets to change optical elements inserted into the optical path. A focal mask turret is at the telescope focal plane, a cold stop mask turret is at the pupil plane just after the collimator lens in the collimated beam, and two filter turrets in the collimated beam section in each branched arm.

Each of the turrets has bump switches for detecting its fiducial position angles and a stepping motor for its rotation. We modified stepping motors P430-258-005 (Portescap) to be applicable for vacuum and cryogenic use by replacing their oiled ball bearings with MoS₂-sputtered dry ball bearings (NTN Corp., Japan).¹

All of the devices are operated by the integrated control system *Motionnet* (Nippon Pulse Motor Co., Ltd.), which consists of a “Center Board” (PPCI-L112) as the main controller on a Windows PC and motor drives (MNET-BCD4020FB), one for each turret unit, cascadingly connected to each other.

In the future extension of the instrument, grism turrets for existing two arms, and a filter and grism turret pairs for another IR arm will be appended.

2.5 Optical Shutter

The optical shutter unit for a CCD imaging is mounted over the optical entrance window of the vacuum chamber (Fig. 7). The unit consists of a black aluminum shutter plate with a rectangular aperture of 151 mm by 97 mm. A linear actuator SACR-S6DH-350BE (SUS Corporation), which equips a linear encoder and an AC servomotor, drives the shutter plate. The shutter plate travels along the long side of the aperture in a single direction at appropriate variable speeds so that the exposure time on the CCD becomes uniform and at intended duration at every positions on the detector. The stability of the exposure time is better than 0.1 msec at the shortest exposure time of 0.3 sec.

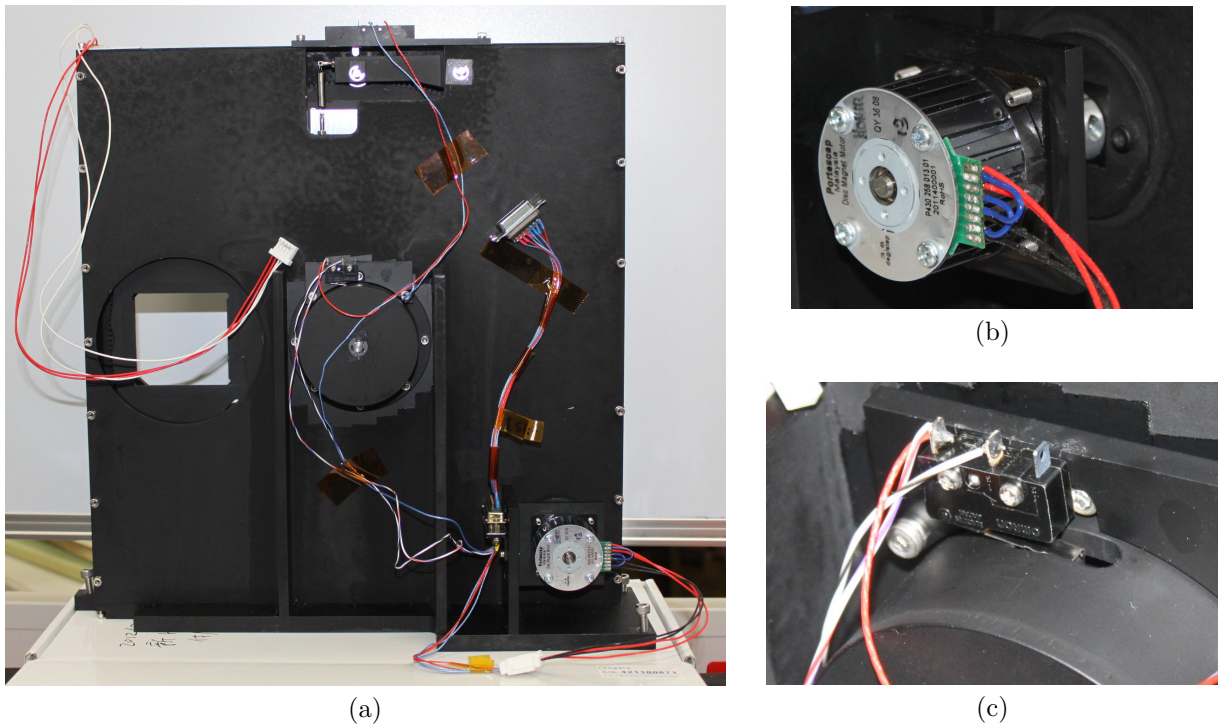


Figure 6. The focal mask turret unit. (a) An overview of the turret unit, (b) the stepping motor, and (c) the bump switch for detecting one of the fiducial position angles.

3. INITIAL OBSERVATIONAL RESULTS

In the most recent test observation of the instrument attached on the Kanata telescope between October 2011 and February 2012, we verified its imaging performance by obtaining images of celestial objects. Fig. 8 shows samples of the images processed by pseudo-color composition. In the central region of an image, the best image size obtained was ~ 0.9 arcsec fwhm at near-infrared bands and ~ 1.7 arcsec fwhm at optical bands, including blurring by seeing effect and telescope tracking error. They are in generally at acceptable level. In the outer region of the field of view, however, apparent blurring and elongation of stellar images were observed. We concluded that this degradation is due to incomplete alignment of the optical elements in the instrument. We are improving it by replacing the lens holding parts and careful adjustment of the optical elements in future.

As a sample of photometric observation, light curves of the young stellar object MM Mon for seven days measured at J, H, and K_s bands are shown in Fig. 9. Every data point was obtained from five dithered frames of 60 sec exposure each. Distinct photometric variations are detected at a photometric precision of about 0.01 mag at J and H bands, and about 0.02 mag at K_s band.

4. SUMMARY AND FUTURE PROSPECTS

We have developed a brand-new instrument HONIR for the 1.5-m Kanata telescope at Higashi-Hiroshima Observatory. HONIR is designed as an imager and spectrograph with a polarimetry function that obtains information of three wavelength bands among optical and near-infrared ranges simultaneously. A imaging function of two wavelength bands ($0.5\text{--}1.0\ \mu\text{m}$ and $1.15\text{--}2.40\ \mu\text{m}$) has been already installed and operated successfully in general so far. The remaining functions (spectroscopy, polarimetry, and another infrared band arm) are under development and will be added in the near future. By using the powerful, multipurpose capabilities of HONIR, we will proceed our observational research on transient or variable astronomical objects at the Kanata telescope further.

ACKNOWLEDGMENTS

We are grateful to S. Sato, S. Sako, K. Okita, Y. Hirahara, M. Kino and K. Yanagisawa for helpful comments and kind cooperation. This research has been supported in part by the Grant-in-Aid for Scientific Research (23244030, 23340048) from the JSPS and MEXT, Japan. Y.M., R.I. and M.S. are supported through the JSPS (Japan Society for the Promotion of Science) Research Fellowship for Young Scientists. Evaluation of performance of the optical elements was supported by Advanced Technology Center, National Astronomical Observatory of Japan.

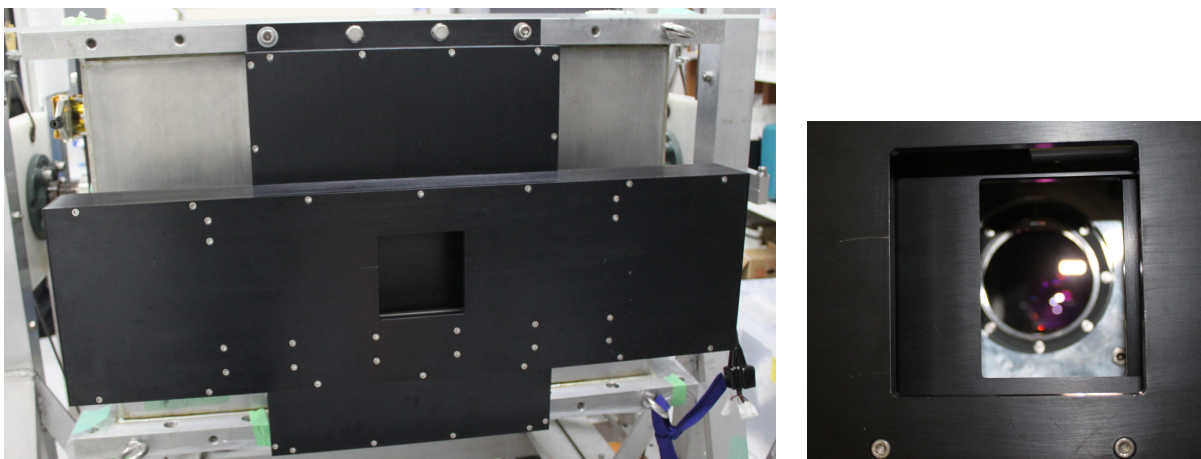


Figure 7. The shutter unit (left) and the aperture on the shutter plate moving over the entrance window across the horizontal direction of the picture (right).

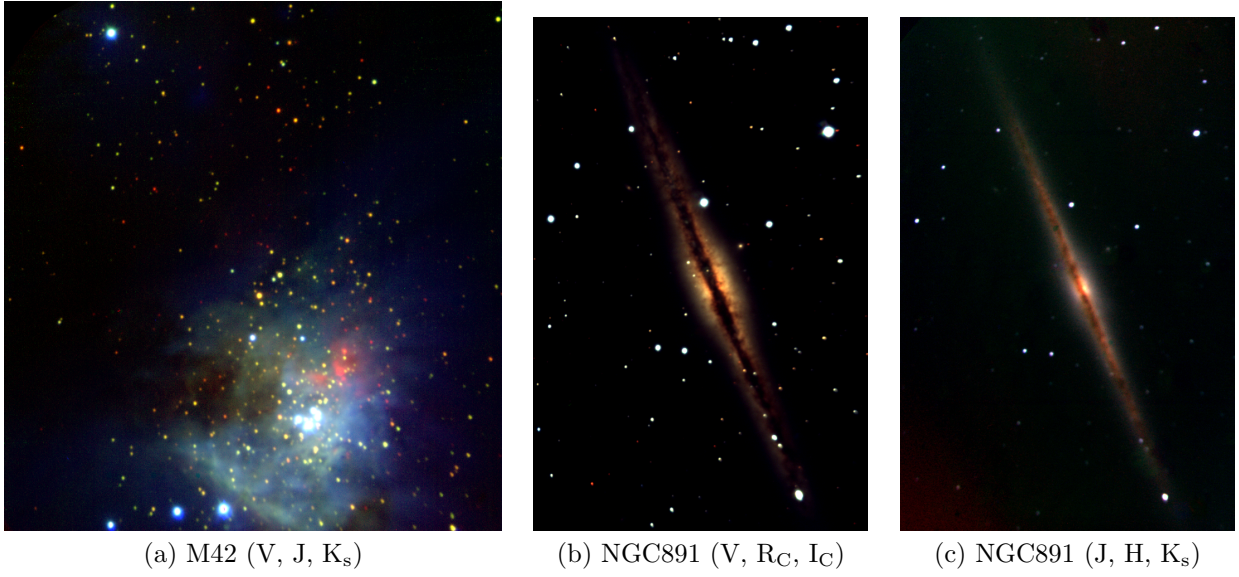


Figure 8. Pseudo-color (blue-green-red) composite images taken by HONIR. (a) M42 ($9'.2 \times 9'.8$; V-band: 20 sec; J-band: 210 sec; K_s-band: 510 sec), (b) NGC891 at optical wavelengths ($6'.2 \times 9'.5$; V-band: 360 sec; R_C-band: 360 sec; I_C-band: 360 sec); and (c) NGC891 at near-infrared wavelengths (J-band: 1200 sec; H-band: 1080 sec; K_s-band: 1080 sec).

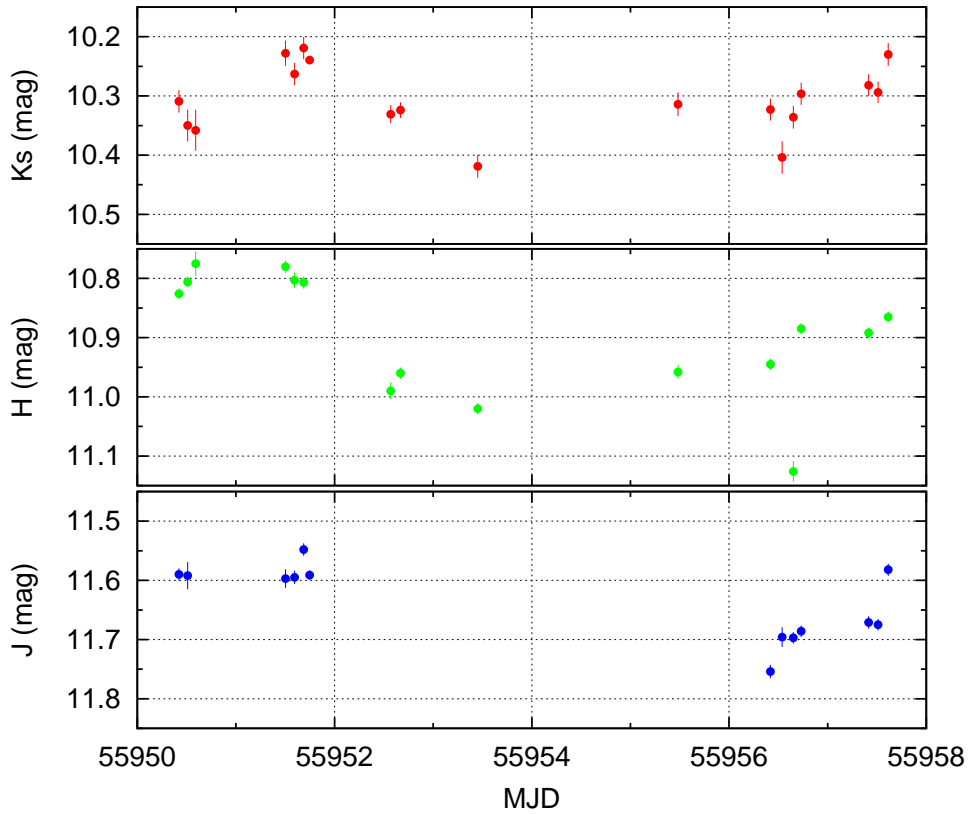


Figure 9. Light curves of the young stellar object MM Mon at J, H, and K_s bands.

REFERENCES

- [1] Watanabe, M., Nakaya, H., Yamamuro, T., Zenno, T., Ishii, M., Okada, M., Yamazaki, A., Yamanaka, Y., Kurita, M., Kino, M., Ijiri, R., Hirao, T., Nagata, T., Sato, S., Kawai, T., Nakamura, Y., Sato, T., Ebizuka, N., Hough, J. H., and Chrysostomou, A., “TRISPEC: A Simultaneous Optical and Near-Infrared Imager, Spectrograph, and Polarimeter,” *Publ. Astron. Soc. Pac.* **117**, 870–884 (2005).
- [2] Kawabata, K. S., Nagae, O., Chiyonobu, S., Tanaka, H., Nakaya, H., Suzuki, M., Kamata, Y., Miyazaki, S., Hiragi, K., Miyamoto, H., Yamanaka, M., Arai, A., Yamashita, T., Uemura, M., Ohsugi, T., Isogai, M., Ishitobi, Y., and Sato, S., “Wide-field one-shot optical polarimeter: HOWPol,” *Proceedings of SPIE* **7014**, 70144L (2008).
- [3] Abdo, A. A., Ackermann, M., Ajello, M., Axelsson, M., Baldini, L., Ballet, J., Barbiellini, G., Bastieri, D., Baughman, B. M., Bechtol, K., and et al., “A change in the optical polarization associated with a γ -ray flare in the blazar 3C279,” *Nature* **463**, 919–923 (2010).
- [4] Sasada, M., Uemura, M., Arai, A., Fukazawa, Y., Kawabata, K. S., Ohsugi, T., Yamashita, T., Isogai, M., Nagae, O., Uehara, T., Mizuno, T., Katagiri, H., Takahashi, H., Sato, S., and Kino, M., “Multiband Photopolarimetric Monitoring of an Outburst of the Blazar 3C 454.3 in 2007,” *Publ. Astron. Soc. Jpn.* **62**, 645–652 (2010).
- [5] Ikejiri, Y., Uemura, M., Sasada, M., Ito, R., Yamanaka, M., Sakimoto, K., Arai, A., Fukazawa, Y., Ohsugi, T., Kawabata, K. S., Yoshida, M., Sato, S., and Kino, M., “Photopolarimetric Monitoring of Blazars in the Optical and Near-Infrared Bands with the Kanata Telescope. I. Correlations between Flux, Color, and Polarization,” *Publ. Astron. Soc. Jpn.* **63**, 639–675 (2011).
- [6] Yamanaka, M., Kawabata, K. S., Kinugasa, K., Tanaka, M., Imada, A., Maeda, K., Nomoto, K., Arai, A., Chiyonobu, S., Fukazawa, Y., Hashimoto, O., Honda, S., Ikejiri, Y., Itoh, R., Kamata, Y., Kawai, N., Komatsu, T., Konishi, K., Kuroda, D., Miyamoto, H., Miyazaki, S., Nagae, O., Nakaya, H., Ohsugi, T., Omodaka, T., Sakai, N., Sasada, M., Suzuki, M., Taguchi, H., Takahashi, H., Tanaka, H., Uemura, M., Yamashita, T., Yanagisawa, K., and Yoshida, M., “Early Phase Observations of Extremely Luminous Type Ia Supernova 2009dc,” *Astrophys. J.* **707**, L118–L122 (2009).
- [7] Uehara, T., Toma, K., Kawabata, K. S., Chiyonobu, S., Fukazawa, Y., Ikejiri, Y., Inoue, T., Itoh, R., Komatsu, T., Miyamoto, H., Mizuno, T., Nagae, O., Nakaya, H., Ohsugi, T., Sakimoto, K., Sasada, M., Tanaka, H., Uemura, M., Yamanaka, M., Yamashita, T., Yamazaki, R., and Yoshida, M., “GRB 091208B: First Detection of the Optical Polarization in Early Forward Shock Emission of a Gamma-Ray Burst Afterglow,” *Astrophys. J.* **752**, L6 (2012).
- [8] Oliva, E., Gennari, S., Vanzi, L., Caruso, A., and Ciofini, M., “Optical materials for near infrared Wollaston prisms,” *Astron. Astrophys. Suppl. Ser.* **123**, 179–182 (1997).
- [9] Perrin, M. D., Graham, J. R., and Lloyd, J. P., “The IRCAL Polarimeter: Design, Calibration, and Data Reduction for an Adaptive Optics Imaging Polarimeter,” *Publ. Astron. Soc. Pac.* **120**, 555–570 (2008).
- [10] Kamata, Y., Miyazaki, S., Nakaya, H., Tsuru, T. G., Takagi, S.-i., Tsunemi, H., Miyata, E., Muramatsu, M., Suzuki, H., and Miyaguchi, K., “Recent results of the fully depleted back-illuminated CCD developed by Hamamatsu,” *Proceedings of SPIE* **6276**, 62761U (2006).
- [11] Nakaya, H., Komiyama, Y., Miyazaki, S., Yamashita, T., Yagi, M., and Sekiguchi, M., “New Focal Plane Array Controller for the Instruments of the Subaru Telescope,” *Publ. Astron. Soc. Pac.* **118**, 478–488 (2006).
- [12] Nakaya, H., Doi, Y., Kamata, Y., Komiyama, Y., and Miyazaki, S., “HyperSuprime: electronics,” *Proceedings of SPIE* **6269**, 62693G (2006).
- [13] Nakaya, H., “CCD Readout Electronics for Subaru Telescope Instruments,” *Publ. Astron. Soc. Pac.* **124**, 485–493 (2012).
- [14] Nakaya, H. and Sato, S., “Multi-array control system for a wide-wavelength observation,” *Proceedings of SPIE* **3354**, 368–372 (1998).
- [15] Sako, S., Aoki, T., Doi, M., Ienaka, N., Kobayashi, N., Matsunaga, N., Mito, H., Miyata, T., Morokuma, T., Nakada, Y., Soyano, T., and K, T., “KWFC: four square degree camera for the Kiso Schmidt Telescope,” *Proceedings of SPIE* **8446**, in this conference (2012).